RAPID COMMUNICATIONS

PHYSICAL REVIEW A VOLUME 39, NUMBER 11 JUNE 1, 1989

Measurements of laser plasma coronal conditions and thermal transport with time-resolved x-ray spectroscopy

O. Willi, S. D. Tabatabaei, and D. Riley
The Blackett Laboratory, Imperial College of Science and Technology, London, SW7 2BZ, United Kingdom

A. Hauer and N. Delamater
Los Alamos National Laboratory, Los Alamos, New Mexico 87545

C. Chenais-Popovics
École Polytechnique, 91128 Palaiseau CEDEX, France

P. Apte and A. Cole
Rutherford Appleton Laboratory, United Kingdom Science Research Council, Chilton, Didcot, Oxfordshire OX11 0QX, United Kingdom
(Received 13 January 1989)

This paper presents a detailed characterization of the plasma conditions near the critical density of a laser-produced plasma. Solid spherical plastic targets with small aluminum tracer dots buried below overcoated plastic layers have been uniformly illuminated with green laser light at irradiances of 10^{14}–10^{15} W/cm^{-2}. Time-resolved temperature and density profiles were obtained by using x-ray emission spectroscopy. Detailed comparisons with hydrodynamic simulations show that the thermal transport is well characterized by a flux limit of 0.1.

In laser-produced plasmas, the laser energy is absorbed below and up to the plasma critical density. The absorbed energy is transported, via electron thermal conduction, beyond the absorption region towards the colder, higher-density region of the target. A knowledge of the plasma conditions close to and above the critical-density surface is, therefore, crucial for an understanding of thermal transport in laser-produced plasmas. Measurements of plasma ablation rates in spherical geometry have indicated that the electron thermal transport is inhibited to 0.05–0.1 with respect to the classical flux streaming limit when compared to hydrodynamic computer simulations.[1–3] These experiments measured the average mass ablation at the ablation layer. No detailed time-resolved observations have, however, been made of the plasma conditions in the region where the transport processes take place.

This Rapid Communication reports on the first detailed time-resolved measurements of the plasma conditions above and close to the critical-density layer of uniformly laser irradiated spherical targets. The temporal histories of the electron density and temperature were obtained via simultaneous time-resolved measurements of x-ray line profiles and line ratios. Temporal resolution of both temperature and density (and spatial resolution of temperature) provide a new diagnostic method for evaluating coronal properties such as transport and ablation. Detailed comparisons of these observations, with hydrodynamic simulations were carried out.

The targets were made of solid plastic, to prevent implosion, and were approximately 150 μm in diameter. Aluminum tracer dots, 0.1 μm thick and ranging from 25 to 75 μm in diameter, were implanted beneath the target surface at depths of 0.24–2.0 μm. The use of microdots has several advantages.[4] First, the emitting source is localized in space and time and so reflects plasma conditions locally. Hydrodynamic simulations indicated that the presence of the dot made no significant difference to the plasma conditions or heat flow. Second, the effect of opacity on line ratios and broadening due to source size are both greatly reduced by using a small source. In addition, the effects of large-scale nonuniformity of irradiance are reduced. In contrast to previous use of tracer dots[4] for measurement of temperature and density, the present work is in an irradiance regime more relevant to laser fusion ($\sim 1\times10^{14}$ W/cm^2) is temporally resolved, and is performed in spherical geometry [where two-dimensional (2D) lateral heat-flow effects are minimized].

Targets were symmetrically irradiated with the twelve beams of the Vulcan Nd-glass laser at the Rutherford Appleton Laboratory High Power Laser Facility. The beams were frequency doubled to 0.53-μm wavelength and had an approximately Gaussian temporal profile with an 800 ps full width at half maximum duration. The focusing on target was tangential with $f/2.5$ lenses. The beam profiles were found to have a 30% rms intensity variation due to small-scale structure. The overlap of the beams and energy imbalance resulted in a 50% peak-to-valley variation over large-scale length. Absorbed irradiances varied from 5×10^{13} to 3×10^{14} W/cm^2.

Several instruments were used to diagnose the x-ray radiation emitted from the heated aluminum tracer dot. The temporal history of the Stark profile for the He-like $1s^2$-$1s4p$ (He$_\gamma$) transition was measured with a novel toroidally focusing pentaerythritol (PET) crystal,[5] which was coupled to an x-ray streak camera to produce a high dispersion spectrum of the line. The time-dependent electron density was obtained from the line profile[6] by com-

paring its shape and width with the RATION and SPECTRA atomic physics codes.[7,8] The observed profile was dominated by Stark broadening early in the pulse since the contribution from Doppler, source and opacity broadening were estimated to be less than 15% of the total width at this time. Spectral and temporal resolutions were 2 mÅ and 50 ps, respectively.

In order to characterize the temperature, the aluminum He-like and H-like resonance lines (1.5–2.5 keV) were recorded with a flat thallium acid phthalate (TlAP) crystal, coupled to a second streak camera to produce a low dispersion spectrum. The line ratio of L_β-to-He_γ was used to obtain the time history of the electron temperature. The special target configuration of a very thin tracer dot made opacity corrections for this line ratio negligible. The spectral and temporal resolutions of the second camera were approximately 10 mÅ and 50 ps, respectively. Both streak cameras observed the target at an angle of 30° from the normal of the microdot plane. All of the x-ray instrumentation was absolutely timed with respect to the heating laser beams, by using a separate laser beam of 100 ps duration to provide an x-ray time fiducial. The time integrated spatial position of the dot was observed with a spatially resolving crystal spectrometer, using a PET or ADP crystal, to record the H-like and He-like resonance lines. The spectrometer was fitted with slits, 10–20 μm wide and placed normal to the aluminum blow-off direction. The spatial resolution achieved was approximately 20 μm. Two x-ray pinhole cameras were used to monitor the uniformity of irradiation. In addition, ion calorimetry was used to measure the absorbed fraction of incident energy.

The experimental observations were compared to simulations carried out with a 1D version of the LASNEX (Ref. 9) Lagrangian hydrodynamic code. The electron thermal transport was modeled by simple group flux-limited diffusion. The code also included non-LTE (local thermodynamic equilibrium) atomic physics, multigroup radiation transport in the diffusion approximation, and ray tracing for the laser deposition. The integrated absorption of the laser energy matched well with the measured values obtained from ion calorimetry.

Figure 1 shows a streak record of the He_γ ($1s^2$-$1s4p$) transition taken on a target which was irradiated at an intensity of 1.4×10^{14} W/cm^2. The aluminum tracer dot was 0.1 μm thick and 75 μm in diameter. The overcoated plastic layer was 0.84-μm thick. The absorbed fraction of energy as measured by ion calorimetry was 46%. A densitometer trace taken 150 ps before the peak of the laser pulse is shown in Fig. 1(b). The measured full width at half maximum is 20 mÅ and is dominated by Stark broadening. A prediction by SPECTRA for the profile was fitted to the experimental results. The best fit was obtained for an electron density of 6×10^{21} cm^{-3}. The electron temperature used in the code was 600 eV (the profile is relatively insensitive to the temperature). The simulations (which model directly the experimental conditions) show that the line emission comes from a highly (1–2 μm) localized spatial region. Thus, the calculation indicates that the measurements are a spatial average over this region.

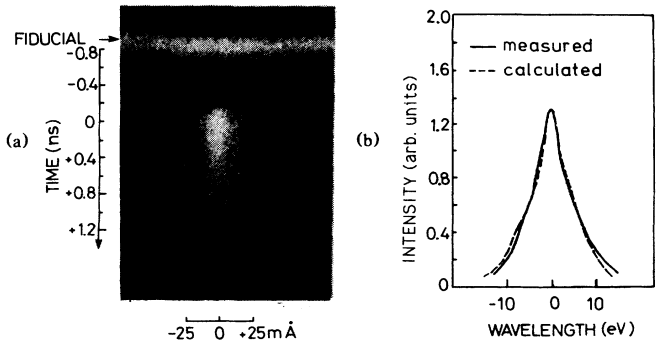

FIG. 1. (a) Streak image of Al He_γ (6.31 Å) transition emitted from the Al tracer dot. (b) Stark profile traced at 150 ps before the peak of the laser pulse and fitted by SPECTRA. Best fit is obtained with an electron density of 6×10^{21}.

The time history of the electron density for the expanding aluminum plasma was obtained in a similar way by taking traces at various times. Figure 2 shows the temporal behavior of the density. The measurements are compared to hydrodynamic simulations. The simulations have been performed using an electron thermal transport flux limiter of 0.1. As can be seen, the predicted density falls off faster at late times than is observed experimentally. At around the peak of the laser pulse, the dot has expanded such that the source broadening becomes comparable to Stark broadening which causes the data to fall off more slowly than the modeling. Deviations between theory and experiment early in the pulse are probably due to inaccuracies in the measurement and timing of the fast rise of the laser pulse. Simulations using a flux limiter of 0.03 give results which deviate from the experimentally measured densities by up to an order of magnitude. Broadband x-ray emission spectra were recorded simultaneously with the high dispersion Stark profiles using another streaked spectrograph. The electron temperature is obtained by taking the ratio of the He_γ ($1s^2$-$1s4p$) and

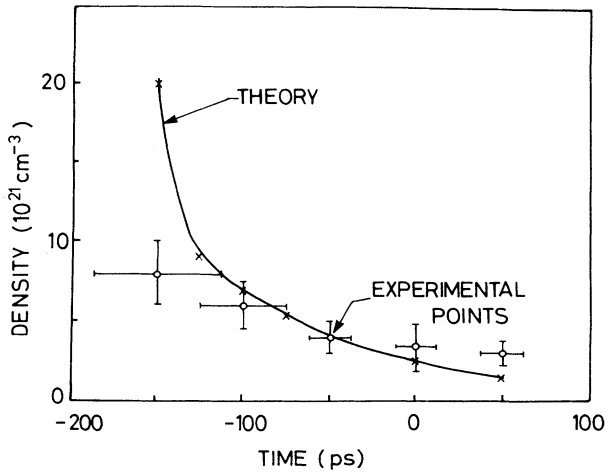

FIG. 2. Measured and calculated electron density profiles of the Al tracer dots as a function of time. Time 0 is the peak of the laser pulse.

L_β ($1s$-$3p$) transitions and then comparing with calculations using the code RATION, which is run for the non-LTE steady-state case. This line ratio is a good temperature diagnostic, being weakly dependent on density and minimally affected by opacity. The temporal history of the electron temperature is obtained by taking the same line ratio at various times. In Fig. 3, the electron temperature is plotted as a function of time. Also shown are the LASNEX predictions for a flux limiter of 0.1. The experimental error bars are due to inaccuracies in the crystal calibration and film noise. This data shows a typical characteristic in that for late times the modeling is falling off more rapidly than the data. More work is needed to refine the modeling for this expanding, recombining phase of the interaction, including 2D hydrodynamic modeling of the blowoff.

Simultaneously with the time-resolved observations, the expansion of the Al dot was studied side-on with a space-resolving crystal spectrograph. The peak of the Al L_β emission was seen at about 25 μm away from the initial position of the dot. Observations with the time resolved spectrograph showed that most of the radiation was emitted during a 300-ps interval centered on the peak of the laser pulse. Consequently, the spatial position of the Al plasma can be compared with the code predictions, and good agreement is found for a flux limiter of 0.1.

A further comparison was made between the experimental data and the hydrodynamic and atomic simulations. Through the use of a time fiducial, an absolute timing of the Al emission was obtained. Consequently, the temporal profile of individual line emission can be directly compared with the code predictions. We show, in Fig. 4, a comparison of the measurement and calculation of the He_γ line. For the calculations, two different assumptions of flux limitation have been made. The calculations were done with a detailed configuration atomic (DCA) physics package[10] that is run in-line with the hydrodynamic simulation. The DCA package calculates time-dependent populations for multiple charge states for arbitrary non-LTE plasmas. The package is coupled self-consistently to the

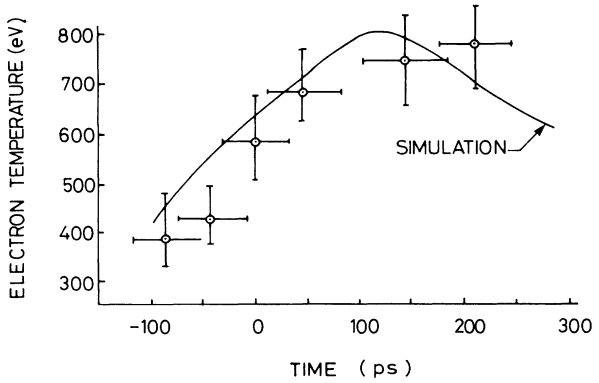

FIG. 3. A determination of temperature from L_β-to-He_γ line ratio, which is quite temperature sensitive in the present regime. We have included a small opacity correction for L_β, as well as a correction for the crystal reflectivity. As can be seen, the agreement with hydrodynamic simulations is good before and near the peak of the laser pulse, but is poorer after the peak.

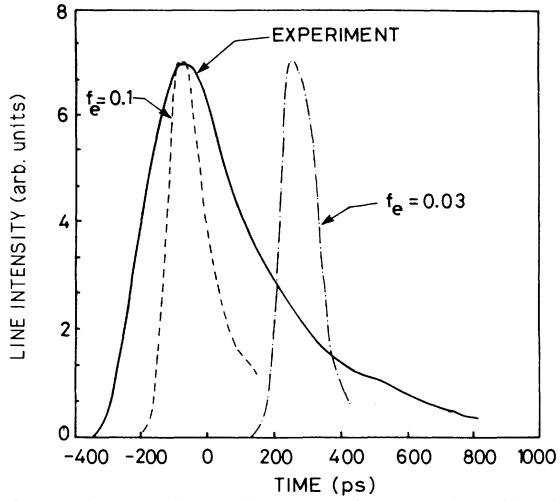

FIG. 4. The experimentally observed temporal profile of the He_γ ($1s^2$-$1s4p$) line is compared with results for different flux limiters in the code. Good agreement is obtained for a flux limiter of 0.1.

hydrodynamic code which uses these quantities in the equation of radiative transport and energy balance. The following processes are included in the model: (1) electron collisional excitation and deexcitation; (2) radiative emission and absorption; (3) electron collisional ionization and photoionization; and (4) radiative, dielectronic, and three body recombination. Thus, this package allows detailed calculation of spectral emission that is particularly appropriate in the diagnosis of the coronal and thermal transport conditions. A good agreement for the peak emission of the helium-like $1s^2$-$1s4p$ line was obtained when a flux limiter of 0.1 was used. For all values of the flux limit the data falls off less rapidly than the simulations, again indicating that more work is needed to model this later phase of expanding plasma.

In conclusion, the use of a small localized tracer dot has greatly reduced the problems of opacity and source broadening and has allowed us to study, in detail, the plasma conditions close to the critical-density region of laser-produced plasmas and to investigate the level of electron thermal transport in the conduction region. Direct measurement of electron density and temperature and observations of the spatial position of the aluminum plasma, during the laser pulse, were compared to hydrodynamic simulations with various flux limiters for the thermal transport with the best agreement being found for $f=0.1$. The use of a newly available, in-line atomic physics package has allowed a direct comparison with the temporally resolved data, again resulting in good agreement if the electron thermal transport is characterized by a flux limiter of 0.1.

We would like to acknowledge the technical support given by the laser and target preparation staff of the Central Laser Facility. Thanks are also due to A. Dyson for software which helped in the automation of the data analysis. We would also like to thank G. Pedicini, R. Gomez, and H. Halbig for valuable assistance in data reduction.

[1]J. A. Tarvin *et al.*, Phys. Rev. Lett. **51**, 1355 (1983).
[2]A. Hauer *et al.*, Phys. Rev. Lett. **53**, 2563 (1984).
[3]T. J. Goldsack, J. D. Kilkenny, B. J. MacGowan, P. F. Cunningham, C. L. S. Lewis, M. H. Key, and P. T. Rumsby, Phys. Fluids **25**, 1634 (1982).
[4]P. G. Burkhalter, M. J. Herbst, D. Duston, J. Gardner, M. Emery, R. R. Whitlock, J. Grun, J. P. Apruzese, and J. Davis, Phys. Fluids **26**, 3650 (1983).
[5]A. Hauer, J. D. Kilkenny, and O. L. Landen, Rev. Sci. Instrum. **56**, 803 (1985).
[6]R. W. Lee, J. D. Kilkenny, R. L. Kauffman, and D. L. Matthews, J. Quant. Spectrosc. Radiat. Transfer **31**, 83 (1984).
[7]R. L. Kauffman, R. W. Lee, D. L. Matthews, and J. D. Kilkenny, J. Quant. Spectrosc. Radiat. Transfer **32**, 335 (1984).
[8]R. W. Lee, B. L. Whitten, and R. E. Stout II, J. Quant. Spectrosc. Radiat. Transfer **32**, 91 (1984).
[9]G. Zimmerman and W. Kruer, Comments Plasma Phys. Controlled Fusion **2**, 85 (1975).
[10]Y. T. Lee, J. Quant. Spectrosc. Radiat. Transfer **38**, 131 (1987).

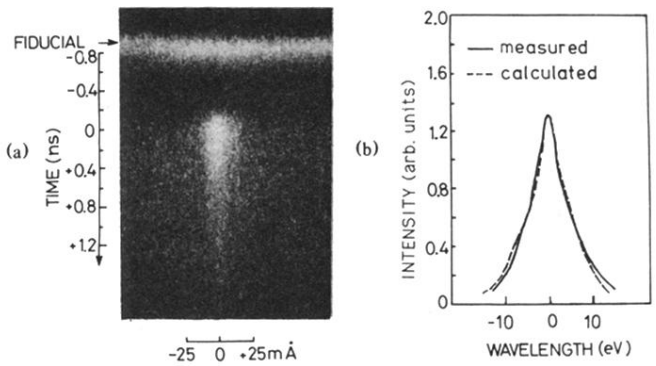

FIG. 1. (a) Streak image of Al He_γ (6.31 Å) transition emitted from the Al tracer dot. (b) Stark profile traced at 150 ps before the peak of the laser pulse and fitted by SPECTRA. Best fit is obtained with an electron density of 6×10^{21}.